telecom

MDPI

Article

Soft Handover via Uplink PD-NOMA in Multi-Beam LEO Satellite Systems

Hulin Li [1,2], Conglu Huang [1], Zhongyu Yang [1] and Yitao Li [1,*]

[1] School of Automation and Information Engineering, Sichuan University of Science and Engineering, Yibin 644000, China; aaron@heltec.cn (H.L.); 324085404507@stu.suse.edu.cn (C.H.); 324085404220@stu.suse.edu.cn (Z.Y.)
[2] Chengdu Heltec Automation Technology Co., Ltd., Chengdu 610000, China
* Correspondence: liyt@mail.ustc.edu.cn

Abstract

Low Earth orbit mobile satellite system (LEO-MSS) is a major system that provides communication support for mobile terminals beyond the coverage of terrestrial communication systems. However, passive handover happens frequently, caused by the quick movement of LEO satellites, making it hard to guarantee quality of service (QoS) for handover users while maintaining a large number of users. To tackle this problem, we propose a novel soft handover scheme and combine it with uplink power-domain non-orthogonal multiple access (PD-NOMA) for the first time to guarantee QoS for handover users and improve uplink throughput. We analyze the uplink PD-NOMA-based soft handover scheme with three users in two beams and give the closed-form expression of the optimal uplink transmission power allocation. Afterward, we introduce this method into a practical multi-beam LEO-MSS system with multiple users and sub-channels and formulate the optimization problems to maximize system throughput. Numerical results show that the proposed uplink PD-NOMA-based soft handover scheme provides much better performance on throughput and fairness for heavy loads.

Keywords: LEO-MSS; uplink collaborative transmission; soft handover; non-orthogonal multiple access (NOMA)

1. Introduction

1.1. Motivation

Compared with terrestrial networks, low Earth orbit mobile satellite systems (LEO-MSSs) can provide wide-area connectivity and complement terrestrial communication infrastructure, particularly in remote and underserved regions [1,2], and satellite communications also play an important role in emergency scenarios [3]. LEO-MSSs differ from terrestrial 5G networks in several aspects, including rapidly varying network topology, propagation delay, Doppler effects, and satellite–ground channel characteristics. The channel model of LEO-ground links makes it hard to achieve full frequency reuse. According to existing work [4], four-color spectra reuse is the best scheme to achieve the largest capacity in LEO-MSS. To further increase the capacity, a smaller coverage radius is needed, which causes more frequent passive handover and difficulties in guaranteeing quality of service (QoS) for handover users. Furthermore, the channel gain of handover users is much smaller than that of non-handover users, making it hard to increase the throughput while guaranteeing QoS for handover users in heavy loads.

Check for updates

Academic Editors: Triantafyllos Kanakis and Charan Litchfield

Received: 1 July 2026
Revised: 29 July 2026
Accepted: 4 August 2026
Published: 6 August 2026

Copyright: © 2026 by the authors. Licensee MDPI, Basel, Switzerland. This article is an open access article distributed under the terms and conditions of the Creative Commons Attribution (CC BY) license.

Soft handover [5,6] and non-orthogonal multiple access (NOMA) [7,8] are promising options to guarantee QoS for handover users and improve system throughput. Although soft handover and NOMA have been studied from different perspectives, their joint design for uplink handover and resource allocation in multi-beam LEO-MSS remains insufficiently explored. The distinct uplink channel characteristics and per-terminal power constraints of LEO-MSS provide a suitable basis for integrating soft handover with PD-NOMA. Accordingly, we propose an uplink PD-NOMA-based soft handover scheme to improve system throughput while guaranteeing QoS for handover users.

1.2. Related Work

Existing studies related to this work mainly involve handover management, cooperative transmission, and NOMA in satellite communication systems. Handover management has been widely investigated to maintain service continuity in highly dynamic LEO satellite networks. An early soft handover solution based on satellite diversity was investigated in [9], where an uplink user could communicate with two satellites during handover. In [10], a forecast-based handover scheme was proposed for an extensible multi-layer LEO-MSS, where handover prediction and dynamic optimization were used to reduce handover delay, signaling cost, and dropping probability. A conditional-handover-based optimization framework was subsequently developed in [11] to improve service continuity and target-satellite selection in LEO-based non-terrestrial networks. More recently, a multi-orbit multi-beam satellite soft handover strategy based on rate-splitting multiple access was developed in [12] to improve communication QoS and spectrum efficiency. These studies show the importance of maintaining continuous connections during satellite mobility and provide a basis for more flexible multi-link transmission during handover.

With the increasing density of LEO constellations, cooperative transmission has also received growing attention. Multi-satellite cooperative communication with asynchronous non-orthogonal transmissions was investigated in [13], where satellite-user association, power allocation, and decoding were jointly considered. A multi-satellite cooperative framework based on joint hybrid beamforming and user scheduling was further developed in [14] to improve the spectral efficiency of ground-user transmission. These studies demonstrate the potential of exploiting multiple satellite links and coordinated resource allocation. In a multi-beam LEO-MSS, the overlapping coverage between adjacent beams similarly provides an opportunity to maintain multiple links for handover users while coordinating the available radio resources.

NOMA provides an additional mechanism for improving resource utilization through non-orthogonal user multiplexing. The applications and potential benefits of PD-NOMA in different satellite architectures were reviewed in [15]. The ergodic capacity of NOMA-based uplink satellite networks under randomly deployed users, imperfect channel state information, and antenna-pointing errors was analyzed in [16]. Code-domain non-orthogonal multiple access (CD-NOMA) distinguishes users through non-orthogonal spreading sequences or codebooks. It can provide code-domain diversity and support overloaded access, showing potential for satellite communication systems [17]. In contrast, PD-NOMA multiplexes users through received-power differences and can be integrated directly with power allocation and SIC-based reception. In the considered uplink soft handover scenario, handover and non-handover users generally experience different channel gains. The handover MT also divides its transmit power between two serving beams. These characteristics make PD-NOMA suitable for the joint transmission and power-allocation design.

Management enables continuous connectivity in highly mobile LEO networks, cooperative transmission exploits multiple available links, and NOMA enables flexible resource

sharing among users. Motivated by these developments, we consider uplink soft handover together with PD-NOMA in a multi-beam LEO-MSS. During handover, an MT maintains connections with two adjacent beams and shares its frequency resources with non-handover users through PD-NOMA. Based on this transmission structure, user association, sub-channel allocation, inter-beam interference, and uplink power allocation are jointly considered to improve system throughput while maintaining QoS for handover users.

1.3. Contributions

In this paper, we focus on the handover problem caused by frequent passive handover in multi-beam LEO satellite systems. We aim at improving the performance of the uplink for handover among different beams in LEO-MSS. Generally, we summarize the contributions of this paper as follows.

- For the first time, we introduce a novel soft handover scheme based on the uplink PD-NOMA in LEO-MSS.
- We analyze the uplink PD-NOMA-based soft handover scheme with three users in two beams and give the closed-form expression of the optimal uplink transmission power allocation.
- We propose an uplink PD-NOMA-based handover resource allocation optimization to maximize uplink throughput in practical multi-beam LEO-MSS with multiple users and bands.
- Simulations were carried out to evaluate the throughput and fairness of the proposed methods compared with existing works. Numerical results show that the proposed methods provide much better performance on throughput and fairness.

The remainder of this paper is structured as follows. In Section 2, the PD-NOMA-based soft handover scheme is introduced. In Section 3, the PD-NOMA-based soft handover problem is formulated in a practical system. Solution techniques and algorithms are proposed in Section 4. Numerical results are presented and discussed in Section 5. Finally, the conclusions and future directions are presented in Section 6.

2. PD-NOMA-Based Soft Handover in LEO-MSS

In LEO-MSS, the power constraint, channel and interference of the uplink are different from those of the downlink. Making full use of this point, we propose a novel soft handover scheme based on the uplink PD-NOMA in LEO-MSS to solve the frequent passive handover problem. The proposed scheme can increase uplink throughput while guaranteeing QoS for handover users. The proposed scheme is introduced first in a scenario of two beams and three users, and it is then extended to a practical system with multiple beams, multiple users and multiple channels.

2.1. LEO Mobile Satellite System

A typical LEO satellite communication system consists of LEO satellites providing multi-beam coverage, ground or gateway stations, and network control entities [2], as shown in Figure 1. A four-color frequency reuse scheme is adopted to reduce the interference among multi-beams.

Passive handover happens frequently in LEO-MSS due to the quick movement of LEO satellites. Handovers in multi-beam LEO-MSS can be divided into beam handover and inter-satellite handover. Letting M be the total number of beams equipped on the LEO satellite, the probability of beam handover is much larger than that of inter-satellite handover as M increases. Therefore, we mainly consider the beam handover in this paper. To achieve seamless coverage, adjacent beams have overlapping coverage regions. An MT located in an overlap region can establish uplink connections with both adjacent beams,

which use different frequency resources. The proposed soft handover scheme considers handover MTs capable of concurrent multi-carrier uplink transmission, allowing them to access the frequency resources associated with the two serving beams simultaneously during the soft handover interval.

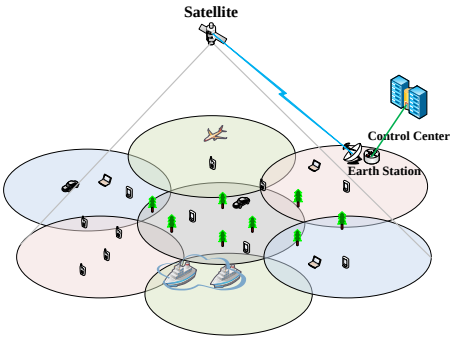


Figure 1. Multi-beam LEO-MSS.

In LEO-MSS, LEO satellites are equipped with directional antennas, and MTs are equipped with omni-directional antennas. Thus, the uplink channel model mainly consists of path loss and atmospheric fading [18]. For MT j located in (x_j, y_j) covered by satellite s, the atmospheric fading is expressed as

$$A(d) = 10^{\left(\frac{3d\chi}{10h}\right)}, \tag{1}$$

where χ is the attenuation through the clouds and rain in dB/km, h is the altitude of the satellites, and d is the propagation distance between the satellites and the MT, given approximately by

$$d = \sqrt{h^2 + (x_j - o_{s,1})^2 + (y_j - o_{s,2})^2}, \tag{2}$$

where $(o_{s,1}, o_{s,2})$ is the position right below a satellite.

The specific expression of the uplink channel gain is given by

$$G = \left(\frac{c_{\text{light}}}{4\pi d f_c}\right)^2 \cdot A(d), \tag{3}$$

where f_c is the carrier frequency, and c_{light} is the speed of light.

The main-lobe gain pattern of the directional aperture antenna is modeled using the cosine-power approximation [19,20] as

$$G_{\text{re}}(\psi) = \mathcal{A}_{\text{eff}} \cos^{\eta}(\psi) \frac{32 \log_{10} 2}{2\left(2 \arccos\left(\sqrt[\eta]{0.5}\right)\right)^2}, \tag{4}$$

where $\mathcal{A}_{\text{eff}}$ is antenna aperture efficiency (assumed to be unity), η is the antenna factor determining the coverage radius, and ψ is the pitch angle. For MT j located in (x_j, y_j) covered by beam i, the pitch angle can be calculated approximately as

$$\psi_{i,j} = 2 \arctan \frac{\sqrt{(x_j - o_{i,1})^2 + (y_j - o_{i,2})^2}}{2h}, \tag{5}$$

where h is the altitude of the satellites, and $(o_{i,1}, o_{i,2})$ is the center position of the coverage region of beam i.

The uplink received power can be expressed as

$$P_{\mathrm{re}} = P_{\mathrm{tr}} \cdot G \cdot G_{\mathrm{re}}, \tag{6}$$

where P_{tr} is the transmission power of MTs.

According to Shannon's formula, the capacity is expressed as

$$C = B\log_2\left(1 + \frac{P_{\mathrm{re}}}{\sum P'_{\mathrm{re}} + \sigma^2}\right), \tag{7}$$

where B is the available spectrum of one sub-channel, $\sum P'_{\mathrm{re}}$ is the total interference from other beams, and σ^2 is the noise power.

In (7), due to the benefit of the directional receiving antenna equipped on LEO satellites, the desired receiving gain of the target user is much larger than the total interference receiving gain according to (4). To maximize uplink throughput, the transmission power P_{tr} should be equal to the largest power $P_{\max}$ according to (7). The uplink respective power constraint at the MTs is different from the downlink total power constraint at the satellite beams. Another difference between the uplink and the downlink lies in the interference. The interference of the downlink depends on the position of the target user and the pointing of the interference beam, while the interference of the uplink depends on the position of the interference user and the pointing of the target beam. These two points make it suitable for the uplink PD-NOMA-based soft handover scheme to apply to LEO-MSS.

2.2. PD-NOMA-Based Soft Handover

Figure 2 illustrates the proposed uplink PD-NOMA-based soft handover scheme in a two-beam scenario with three users. MT a and MT b are served by beam 1 and beam 2 using bandwidths B_1 and B_2, respectively. During soft handover, MT c maintains uplink connections with both beams and shares the corresponding frequency resources with MT a and MT b through PD-NOMA. Specifically, MT c transmits over B_1 toward beam 1 together with MT a, and it transmits over B_2 toward beam 2 together with MT b. During concurrent transmission, the transmit power of MT c is divided between the two uplink links subject to its total uplink power constraint.

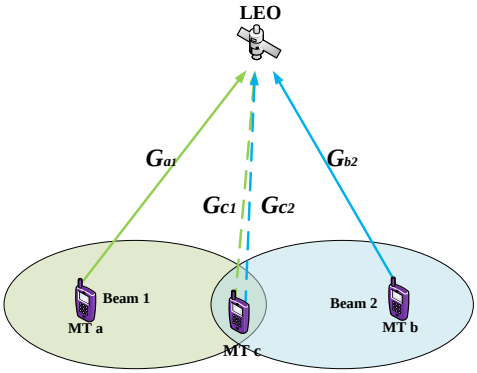


Figure 2. PD-NOMA -based soft handover.

Without PD-NOMA-based soft handover, the uplink rates of MT a and MT b are expressed as

$$\tilde{R}_a = B_1\log_2\left(1 + \frac{P_{a1}G_{a1}}{\sigma^2}\right) \tag{8}$$

and

$$\tilde{R}_b = B_2\log_2\left(1 + \frac{P_{b2}G_{b2}}{\sigma^2}\right), \tag{9}$$

respectively, where G_{a1} and G_{b2} denote the channel gains from MT a and MT b to beam 1 and beam 2, respectively. P_{a1} and P_{b2} denote their corresponding transmit powers, while B_1 and B_2 denote the allocated bandwidths.

After introducing the PD-NOMA-based soft handover, successive interference cancellation (SIC) [21] is employed at the satellite receiver for signal detection. The received signals on B_1 and B_2 are processed separately. On B_1, the satellite first decodes the signal of MT a, subtracts it from the received signal, and then decodes the signal of the handover MT c. Similarly, on B_2, the signal of MT b is decoded and canceled before decoding the signal of MT c. Each sub-channel, therefore, forms a two-user PD-NOMA group and requires only one SIC cancellation stage. In the multi-user extension, additional two-user groups are formed through sub-channel allocation and user pairing, while the SIC depth on each sub-channel remains unchanged. Therefore, the uplink rates of MT a and MT b are expressed as

$$R_{a1} = B_1 \log_2 \left(1 + \frac{P_{a1} G_{a1}}{P_{c1} G_{c1} + \sigma^2}\right) \tag{10}$$

and

$$R_{b2} = B_2 \log_2 \left(1 + \frac{P_{b2} G_{b2}}{P_{c2} G_{c2} + \sigma^2}\right), \tag{11}$$

respectively, where G_{c1} and G_{c2} are the channel gains from the handover MT c to the satellite beams 1 and 2. P_{c1} and P_{c2} are the transmission power of the handover MT c in bandwidth B_1 and B_2 respectively. The sum rate of the handover MT is expressed as

$$R_c = B_1 \log_2 \left(1 + \frac{P_{c1} G_{c1}}{\sigma^2}\right) + B_2 \log_2 \left(1 + \frac{P_{c2} G_{c2}}{\sigma^2}\right). \tag{12}$$

Thus, the sum rate after introducing PD-NOMA-based soft handover is expressed as

$$R_{\text{sum}} = R_{a1} + R_{b2} + R_c. \tag{13}$$

Therefore, the sum rate improvement of PD-NOMA-based soft handover is expressed as

$$\Delta R = R_{\text{sum}} - \tilde{R}_a - \tilde{R}_b. \tag{14}$$

To maximize the sum rate, P_{c1} and P_{c2} should be allocated optimally. To simplify the formula derivation, letting $\sigma^2 = 1$ normalize the noise power and the received power, $B_1 = B_2 = 1$ and $P_{a1} = P_{b2} = P_{c1} + P_{c2} = P_{\max}$, the sum rate $R_{\text{sum}}(P_{c1})$ is expressed as

$$\begin{aligned} R_{\text{sum}}(P_{c1}) = {} & \log_2 \left\{ \left(1 + \frac{P_{\max} G_{a1}}{P_{c1} G_{c1} + 1}\right)(1 + P_{c1} G_{c1})[1 + (P_{\max} - P_{c1}) G_{c2}] \left[1 + \frac{P_{\max} G_{b2}}{(P_{\max} - P_{c1}) G_{c2} + 1}\right] \right\} \\ = {} & \log_2 \{ -G_{c1} G_{c2} P_{c1}^2 + [G_{c1} - G_{c2} + (G_{c1} G_{c2} + G_{c1} G_{b2} - G_{c2} G_{a1}) P_{\max}] P_{c1} \\ & + 1 + (G_{c2} + G_{a1} + G_{b2}) P_{\max} + G_{a1} (G_{b2} + G_{c2}) P_{\max}^2 \} \end{aligned} \tag{15}$$

Letting

$$\frac{\partial R_{\text{sum}}}{\partial P_{c1}^*} = 0, \tag{16}$$

we get the optimal allocated transmission power P_{c1}^* as

$$P_{c1}^* = \frac{G_{c1} - G_{c2} + (G_{c1} G_{c2} + G_{c1} G_{b2} - G_{c2} G_{a1}) P_{\max}}{2 G_{c1} G_{c2}}. \tag{17}$$

Therefore, the maximal sum rate $R_{\text{sum}}(P_{c1}^*)$ is expressed as

$$\begin{aligned} R_{\text{sum}}(P_{c1}^*) &= \log_2\{\frac{[G_{c1}-G_{c2}+(G_{c1}G_{c2}+G_{c1}G_{b2}-G_{c2}G_{a1})P_{\max}]^2}{4G_{c1}G_{c2}} \\ &\quad +1+(G_{c2}+G_{a1}+G_{b2})P_{\max}+G_{a1}(G_{b2}+G_{c2})P_{\max}^2\} \\ &= \log_2\{\frac{(G_{c1}+G_{c2})^2}{4G_{c1}G_{c2}}+\frac{(2G_{c1}+2G_{c2}+2G_{a1}G_{b2}P_{\max}+G_{c1}G_{c2}P_{\max})P_{\max}}{4} \\ &\quad +\frac{{G_{c2}}^2{G_{a1}}^2P_{\max}^2+\left(2G_{c1}G_{c2}P_{\max}+2{G_{c2}}^2P_{\max}+2G_{c1}{G_{c2}}^2P_{\max}^2\right)G_{a1}}{4G_{a2}G_{b2}} \\ &\quad +\frac{{G_{c1}}^2{G_{b2}}^2P_{\max}^2+\left(2G_{c1}G_{c2}P_{\max}+2{G_{c1}}^2P_{\max}+2{G_{c1}}^2G_{c2}P_{\max}^2\right)G_{b1}}{4G_{a2}G_{b2}}\} \end{aligned} \tag{18}$$

In a practical system, the signal-to-interference plus noise ratio (SINR) should be larger than the threshold ε to decode the data successfully at the receiver via the adopted modulation and coding scheme (MCS). Thus, P_{c1} should satisfy the following constraints (the constraints of SINR can be replaced by the constraints of satisfying the minimum rate of users because they are equivalent in the final expression of the value ranges).

$$P_{c1}G_{c1} \geq \varepsilon \tag{19a}$$

$$(P_{\max}-P_{c1})G_{c2} \geq \varepsilon \tag{19b}$$

$$\frac{P_{a1}G_{a1}}{P_{c1}G_{c1}+1} \geq \varepsilon \tag{19c}$$

$$\frac{P_{b2}G_{b2}}{P_{c2}G_{c2}+1} \geq \varepsilon \tag{19d}$$

Thus, we get the feasible value range of P_{c1}^* as follows (if P_{c1} does not have a solution in the range, MT c cannot be selected as a soft handover user).

$$P_{c1}^* \leq \min\{1-\frac{\varepsilon}{G_{c2}}, \frac{P_{a1}G_{a1}-\varepsilon}{G_{c1}\varepsilon}\} \tag{20a}$$

$$P_{c1}^* \geq \max\{\frac{\varepsilon}{G_{c1}}, 1+\frac{\varepsilon-P_{b2}G_{b2}}{\varepsilon G_{c2}}\} \tag{20b}$$

The optimal power P_{c1}^* is determined by Equations (17), (20a), and (20b).

The two-beam three-user scenario analyzed above provides the basic model for the proposed PD-NOMA-based soft handover scheme. In a practical system with multiple users and sub-channels, multiple PD-NOMA user pairs can be formed across different beams and sub-channels. As the system scale increases, user association, sub-channel pairing, inter-beam interference, and power allocation become coupled. Therefore, joint resource allocation is required to maximize system throughput. The corresponding multi-beam, multi-user, and multi-sub-channel system is formulated in the following section.

3. Problem Formulation

Based on the basic PD-NOMA soft handover unit analyzed in Section 2.2, we now extend the framework to a practical system with multiple beams, multiple users, and multiple sub-channels. As the number of users increases, the candidate user associations and sub-channel pairings increase, while multiple simultaneously active links introduce additional inter-beam interference. Therefore, joint user association, sub-channel alloca-

tion, and power allocation are required to maximize system throughput. The resulting optimization problem is formulated as OP0.

$$\begin{aligned}
&\text{OP0} \quad \max \quad \Re \\
&\text{s.t.} \\
&\text{C1}: \sum_{j} a_{i,j} = \tfrac{K}{4}, && \forall\, i \\
&\text{C2}: \sum_{i=1}^{I} a_{i,j} = 1, && \forall\, j \\
&\text{C3}: a_{i,j} \in \{0,1\}, && \forall\, i,j \\
&\text{C4}: \sum_{m} b_{i,m} = \tfrac{K}{4}, && \forall\, i \\
&\text{C5}: \sum_{i=1}^{I} b_{i,m} = 2, && \forall\, m \\
&\text{C6}: b_{i,m} \in \{0,1\}, && \forall\, i,m \\
&\text{C7}: P_{m,k1} + P_{m,k2} \le P_{\max}, && \forall\, m,k \\
&\text{C8}: 0 \le P_j \le P_{\max}, && \forall\, j \\
&\text{C9}: \text{SINR}_j \ge \varepsilon,\ \text{SINR}_m \ge \varepsilon, && \forall\, j,m
\end{aligned} \tag{21}$$

where $\Re$ is the system throughput, and K is the total number of sub-channel number in the system. $P_{\max}$ is the maximum power constraint for uplink users. Notations of the subscripts are shown in Table 1. C1 to C3 are the constraints of the sub-channel resource for non-handover users. C4 to C6 are the constraints of the sub-channel resource for handover users. C7 is the power constraint of the handover users. C8 is the power constraint of the non-handover users.

OP0 is too complicated to obtain solutions. Thus, we found a step-by-step approach to get a practical solution. We create the user classification and association first to distinguish handover users and non-handover users for all beams. Then, we allocate sub-channels for non-handover users to minimize the interference. Finally, we match sub-channels and allocate powers for handover users to maximize the throughput.

Table 1. Notations.

Notations	Meanings
k	Sub-channel index
i	Beam index
j	Non-handover user index
m	Handover user index
P	Uplink power
G	Uplink channel gain

3.1. Dynamic User Association and Allocation for Non-Handover Users

According to the user locations and channel gains, we achieve user classification and association based on the handover forecast model. The user association and pairing in four-color beams are illustrated in Figure 3.

Non-handover users are associated with one beam, and handover users are associated with two beams. Users are associated with the beam and allocated sub-channel resources according to the channel gain. For all non-handover users $j \in \{1, 2, \ldots J\}$, by letting $\boldsymbol{A}_{I\times J} = [a_{i,j}]$ be the association and allocation results, the problem is formulated as OP1.

$$\begin{aligned} \text{OP1} \quad & \max \quad \sum_{i=1}^{I}\sum_{j=1}^{J} a_{i,j}G_{j,i} \\ \text{s.t.} \quad \text{C1}: \quad & \sum_{i=1}^{I} a_{i,j} = 1, \quad \forall \ j \\ \text{C2}: \quad & \sum_{j=1}^{J} a_{i,j} \le K_i, \quad \forall \ i \\ \text{C3}: \quad & a_{i,j} \in \{0,1\}, \quad \forall \ i,j \end{aligned} , \tag{22}$$

where $G_{j,i}$ is the channel gain from user j to beam i, K_i is the total bandwidth of beam i, and $a_{i,j} = 1$ refers to allocate sub-channel resource to user j in beam i. OP1 is a zero–one integer linear programming problem.

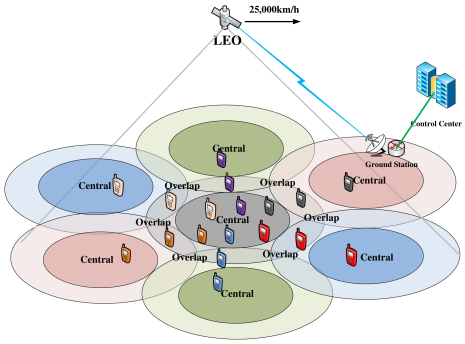


Figure 3. User association and pairing in four-color beams.

3.2. Dynamic User Association and Allocation for Handover Users

For all handover users $m \in \{1, 2, \ldots, M\}$, by letting $\boldsymbol{B}_{I\times M} = [b_{i,m}]$ be the association results, the problem is formulated as OP2.

$$\begin{aligned} \text{OP2} \quad & \max \quad \sum_{i=1}^{I}\sum_{m=1}^{M} b_{i,m}G_{m,i} \\ \text{s.t.} \quad \text{C1}: \quad & \sum_{i=1}^{I} b_{i,m} = 2, \quad \forall \ m \\ \text{C2}: \quad & \sum_{m=1}^{M} b_{i,m} \le K_i, \quad \forall \ i \\ \text{C3}: \quad & b_{i,m} \in \{0,1\}, \quad \forall \ i,m \end{aligned} , \tag{23}$$

where $G_{m,i}$ is the channel gain from user m to beam i, and $b_{i,m} = 1$ refers to allocating sub-channel resources to user m in beam i. OP2 is also a zero–one integer linear programming problem.

3.3. Sub-Channel Allocation for Non-Handover Users

To maximize the throughput, the MTs allocated with sub-channels should use the maximum power for uplink transmission. Thus, the problem is to find the optimal sub-channel allocation for all MTs. For an N color frequency reuse system, the available sub-channels for beam i is

$$\left(\frac{K}{N}(i \bmod N) + 1, \ldots, \frac{K}{N}[(i \bmod N) + 1]\right) \tag{24}$$

where K is the total sub-channels of this system. Letting $k_i = \frac{K}{N}(i \bmod N) + k, k \le \frac{K}{N}$, for MT j covered by beam i, the rate on the sub-channel k is

$$\begin{aligned} R_{j,k,i} &= B\log_2\left(1+\mathrm{SINR}_{j,k,i}\right) \\ &= B\log_2\left(1+\frac{P_{j,k}G_{j,i}}{\sum\limits_{j'\neq j}^{J} P_{j',k}G_{j',i}+\sigma^2}\right), \end{aligned} \tag{25}$$

where B is the bandwidth, $P_{j,k}$ is the transmission power of MT j on the sub-channel k, and $G_{j,i}$ is the channel gain from MT j to beam i. The throughput for all non-handover users is

$$\Re_J = \sum_i \sum_j \sum_k R_{j,k,i}. \tag{26}$$

Therefore, the problem is formulated as OP3.

$$\begin{aligned} &\mathrm{OP3} \quad \max \quad \Re_J \\ \text{s.t.} \quad &\mathrm{C1}: \quad 0 \le \sum_k P_{j,k} \le P_{\max}, \quad \forall j \\ &\mathrm{C2}: \quad 0 \le \sum_j P_{j,k} \le P_{\max}, \quad \forall k \\ &\mathrm{C3}: \quad P_{j,k} \in \{0, P_{\max}\}, \quad \forall k, j \end{aligned}, \tag{27}$$

OP3 is a zero–one fractional programming program.

3.4. Sub-Channel and Power Allocation for Handover Users

$$R_{j,k,i} = B\log_2\left(1+\mathrm{SINR}_{j,k,i}\right) = B\log_2\left(1+\frac{P_{j,k}G_{j,i}}{\sum\limits_{j'\neq j}^{J} P_{j',k}G_{j',i} + \sum\limits_{i=1}^{I}\sum\limits_{m=1}^{M} P_{m,k}G_{m,i}+\sigma^2}\right) \tag{28}$$

$$R_{m,k,i} = s_{m,k,i}B\log_2(1+\mathrm{SINR}_{m,k,i}) = s_{m,k,i}B\log_2\left(1+\frac{P_{m,k}G_{m,i}}{\sum\limits_{i'\neq i}^{I}\left(\sum\limits_{m'\neq m}^{M} P_{m',k}G_{m',i} + \sum\limits_{j'\neq j}^{J} P_{j',k}G_{j',i}\right)+\sigma^2}\right) \tag{29}$$

After introducing soft handover users, the rate of non-handover user j covered by beam i on the sub-channel k is updated, as per (28), where $P_{m,k}$ is the transmission power of MT m on the sub-channel k, and $G_{m,i}$ is the channel gain from MT m to beam i.

Letting $\boldsymbol{S} = [s_{m,k,i}]$ be the sub-channel allocation results for handover users, where $s_{m,k,i}$ is the sub-channel allocation results for handover user m at sub-channel k served by beam i, the rate of handover user m on the sub-channel k covered by beam i is expressed as in (29).

The total rate for the handover user m is given by

$$R_m = R_{m,k1,i1} + R_{m,k2,i2}, \tag{30}$$

where $i1$ and $i2$ are the two beams allocating resources to handover user m for soft handover. $k1$ and $k2$ are the allocated sub-channels for handover user m.

The throughput of all handover users is given by

$$\Re_M = \sum_{m=1}^{M} R_m. \tag{31}$$

The throughput of this system is expressed as

$$\Re = \Re_J + \Re_M. \tag{32}$$

Thus, to maximize the throughput of this system, the problem of sub-channel and power allocation for handover users is formulated as OP4.

$$\begin{aligned} \text{OP4} \quad & \max \quad \Re \\ \text{s.t.} \quad & \text{C1}: \sum_{k} s_{m,k,i} = b_{i,m}, \quad \forall\, i, m \\ & \text{C2}: \sum_{m=1}^{M} s_{m,k,i} \le 1, \quad \forall\, i, k \\ & \text{C3}: s_{m,k,i} \in \{0,1\}, \quad \forall\, m, i, k \\ & \text{C4}: \sum_{i=1}^{I} \sum_{k} s_{m,k,i} P_{m,k} = P_{\max}, \quad \forall\, m \\ & \text{C5}: 0 \le P_{m,k} \le P_{\max}, \quad \forall\, m, k \\ & \text{C6}: \text{SINR}_j \ge \varepsilon, \text{SINR}_m \ge \varepsilon, \quad \forall\, j, m \end{aligned} \tag{33}$$

4. Solution Techniques and Algorithms

OP1 and OP2 are zero–one integer linear programming problems and can be solved via the sort-based implicit enumeration algorithm [22]. OP3 is a zero–one fractional programming problem and can be solved by the Dinkelbach algorithm [23,24] within a logarithmic complexity. In this section, we will focus on how to obtain the solutions of OP4.

4.1. Sub-Channel Allocation

In this subsection, we introduce a simplified solution according to the optimal power allocation results in Section 2.2. The results give the optimal uplink power allocation for the handover users in two given sub-channels, so we only need to find the optimal sub-channel allocation results for handover users. Thus, OP4 can be simplified as OP5.

$$\begin{aligned} \text{OP5} \quad & \max \quad \Re \\ \text{s.t.} \quad & \text{C1}: \sum_{k} s_{m,k,i} = b_{i,m}, \quad \forall\, i, m \\ & \text{C2}: \sum_{m=1}^{M} s_{m,k,i} \le 1, \quad \forall\, i, k \\ & \text{C3}: s_{m,k,i} \in \{0,1\}, \quad \forall\, m, k, i \end{aligned} \tag{34}$$

OP5 is also a zero–one integer linear programming problem, used to get the optimal sub-channel allocation; it can be solved using the sort-based implicit enumeration method [22].

The power allocation in Section 2.2 does not consider the interference from users covered by other beams. Therefore, the method in this subsection can provide sub-optimal power allocation via a low-complexity algorithm, which can be easily carried out at the satellites in the practical LEO-MSS.

4.2. Power Allocation

Section 4.1 provides a low-complexity solution to get optimal sub-channel allocation and sub-optimal power allocation without considering interference. In this subsection, we will provide the method with which to get the optimal power allocation for handover users after considering the interference in the system with multiple beams, multiple users and multiple channels. The problem is formulated as OP6.

$$\begin{aligned} &\text{OP6} \quad \max \quad \Re \\ &\text{s.t.} \quad \text{C1}: P_{k1,m} + P_{k2,m} = P_{\max}, \quad \forall\, m \\ &\qquad \text{C2}: 0 \le P_{k,m} \le P_{\max}, \quad \forall\, m,k \\ &\qquad \text{C3}: \text{SINR}_j \ge \varepsilon, \text{SINR}_m \ge \varepsilon, \quad \forall\, j,m \end{aligned} \tag{35}$$

OP6 is a non-convex, fractional programming problem. We use the Lagrangian dual method to find the optimal results.

The Lagrangian function of OP6 is

$$\begin{aligned} L(P_{m,k,i},\lambda,\mu,\nu,\tau) &= \sum_{i=1}^{I}\sum_{k=1}^{K}(R_{j,k,i}+R_{m,k,i}) \\ &+ \sum_{i=1}^{I}\sum_{k=1}^{K}\lambda_{m,k,i}(\text{SINR}_{j,k,i}-\varepsilon) \\ &+ \sum_{i=1}^{I}\sum_{k=1}^{K}\mu_{m,k,i}(\text{SINR}_{m,k,i}-\varepsilon) \\ &+ \sum_{i=1}^{I}\sum_{k=1}^{K}\nu_{m,k,i}(P_{\max}-P_{m,k,i}) \\ &+ \sum_{i=1}^{I}\sum_{k=1}^{K}\tau_{m,k,i}P_{m,k,i} \end{aligned} , \tag{36}$$

where $\lambda,\mu,\nu,\tau \ge 0$ are the Lagrangian dual variables. The Lagrangian equation of OP6 is

$$h(\lambda,\mu,\nu,\tau) = \sup_{P_{m,k,i}\ge 0} L(P_{m,k,i},\lambda,\mu,\nu,\tau). \tag{37}$$

The dual problem of OP6 is

$$\min_{(\lambda,\mu,\nu,\tau)\ge 0} h(\lambda,\mu,\nu,\tau). \tag{38}$$

$L(P_{m_{i_n},k_n},\lambda,\mu,\nu,\tau)$ is a convex function when $P_{m_{i_n},k_n} \ge 0$.

Since OP5 has achieved user pairing to reduce interference and increase throughput, the interference from handover users to the other beams is very small. Thus, the approximate KKT condition is given as

$$\begin{aligned} \frac{\partial L}{\partial P_{m,k}} &= \frac{G_{m,i}}{\sum_{i'\ne i}\sum_{j'\ne j}^{J} P_{j',k}G_{j',i}+P_{m,k}G_{m,i}+\sigma^2} \\ &+ \frac{P_{j,k}G_{j,i}G_{m,i}\lambda_{m,k,i}}{\left(\sum_{i'\ne i}\sum_{j'\ne j}^{J} P_{j',k}G_{j',i}+P_{m,k}G_{m,i}+\sigma^2\right)^2} \\ &+ \frac{G_{m,i}\mu_{m,k,i}}{\sum_{i'\ne i}\sum_{j'\ne j}^{J} P_{j',k}G_{j',i}+\sigma^2} - \nu_{m,k,i} + \tau_{m,k,i} = 0 \end{aligned} . \tag{39}$$

Letting

$$P_g = \left(\sum_{i'\ne i}\sum_{j'\ne j}^{J} P_{j',k}G_{j',i} + P_{m,k}G_{m,i} + \sigma^2\right)^{-1}, \tag{40}$$

(39) can be expressed as

$$\frac{\partial L}{\partial P_{m,k}} = P_{j,k}G_{j,i}G_{m,i}\lambda_{m,k,i}{P_g}^2 + G_{m,i}P_g + \frac{G_{m,i}\mu_{m,k,i}}{\sum_{i'\ne i}\sum_{j\ne j}^{J} P_{j',k}G_{j',i}+\sigma^2} - \nu_{m,k,i} + \tau_{m,k,i} = 0. \tag{41}$$

We get P_g as

$$P_g = \frac{\sqrt{{G_{m,i}}^2 - 4P_{j,k}G_{j,i}G_{m,i}\lambda_{m,k,i}\left(\frac{G_{m,i}\mu_{m,k,i}}{\sum_{i'\neq i}\sum_{j'\neq j}^{J} P_{j',k}G_{j',i}+\sigma^2} - \nu_{m,k,i} + \tau_{m,k,i}\right)} - G_{m,i}}{2P_{j,k}G_{j,i}G_{m,i}\lambda_{m,k,i}} \tag{42}$$

Thus, we get the optimal transmission powers as

$$P^*_{m,k} = \frac{{P_g}^{-1} - \sum_{i'\neq i}\sum_{j'\neq j}^{J} P_{j',k}G_{j',i} - \sigma^2}{G_{m,i}}. \tag{43}$$

The Lagrangian equation is expressed as

$$\begin{aligned} & h(\lambda,\mu,\nu,\tau) \\ &= \sup_{P_{m,k}\geq 0} L(P_{m,k},\lambda,\mu,\nu,\tau) \\ &= \sup_{P_{m,k}\geq 0} \sum_{i=1}^{I}\sum_{k=1}^{K}(R^*_{j,k,i} + R^*_{m,k,i}) \\ &+ \sum_{i=1}^{I}\sum_{k=1}^{K}\lambda_{m,k,i}(\mathrm{SINR}^*_{j,k,i} - \varepsilon) \\ &+ \sum_{i=1}^{I}\sum_{k=1}^{K}\mu_{m,k,i}(\mathrm{SINR}^*_{m,k,i} - \varepsilon) \\ &+ \sum_{i=1}^{I}\sum_{k=1}^{K}\nu_{m,k,i}(P_{\max} - P^*_{m,k}) \\ &+ \sum_{i=1}^{I}\sum_{k=1}^{K}\tau_{m,k,i}P^*_{m,k} \end{aligned} . \tag{44}$$

The dual problem of OP6 is

$$\min_{(\lambda,\mu,\nu,\tau)\geq 0} h(\lambda,\mu,\nu,\tau), \tag{45}$$

where $h(\lambda,\mu,\nu,\tau)$ is a convex function. We use the gradient descent method [25] to solve it. The partial derivatives are

$$\frac{\partial h}{\partial \lambda_{m,k,i}} = \mathrm{SINR}^*_{j,k,i} - \varepsilon, \tag{46}$$

$$\frac{\partial h}{\partial \mu_{m,k,i}} = \mathrm{SINR}^*_{m,k,i} - \varepsilon, \tag{47}$$

$$\frac{\partial h}{\partial \nu_{m,k,i}} = P_{\max} - P^*_{m,k} \tag{48}$$

and

$$\frac{\partial h}{\partial \tau_{m,k,i}} = P^*_{m,k}. \tag{49}$$

Thus, we get

$$\begin{aligned} \lambda_{m,k,i}(l+1) &= \left[\lambda_{m,k,i}(l) - \beta^{m,k,i}_{\lambda}(l)\frac{\partial h}{\partial \lambda_{m,k,i}}(l)\right]^+ \\ \mu_{m,k,i}(l+1) &= \left[\mu_{m,k,i}(l) - \beta^{m,k,i}_{\mu}(l)\frac{\partial h}{\partial \mu_{m,k,i}}(l)\right]^+ \\ \nu_{m,k,i}(l+1) &= \left[\nu_{m,k,i}(l) - \beta^{m,k,i}_{\nu}(l)\frac{\partial h}{\partial \nu_{m,k,i}}(l)\right]^+ \\ \tau_{m,k,i}(l+1) &= \left[\tau_{m,k,i}(l) - \beta^{m,k,i}_{\tau}(l)\frac{\partial h}{\partial \tau_{m,k,i}}(l)\right]^+ \end{aligned}, \tag{50}$$

where $[x]^+ \equiv \max\{0, x\}$, $l \in \{1, 2, \ldots, l_{\max}\}$ is the iteration index. $\beta(l) = \beta(1)/l$ is the step length.

4.3. Contrast Solution

Via Sections 4.1 and 4.2, we provide the solution results of OP4 stepwise by sub-channel and power allocation. However, it is hard to prove that the results of this two-step method are the global optimal solution. Thus, we introduce an exhaustive heuristic method based on the genetic algorithm [26,27] to make comparisons. The precision of the power is $P_{\max}/32$, and the complexity is $O((NI_n)^2 L N_g)$, where L is the maximum iterations, and N_g is the original individual number.

4.4. Proposed Algorithms

All the designed algorithms are run on LEO satellites. The sort-based implicit enumeration algorithm for OP1 is shown in Algorithm 1, whose complexity is $O(JK_i)$. The sort-based implicit enumeration algorithm for OP2 is shown in Algorithm 2, whose complexity is a bit more than $O(MK_i)$.

Algorithm 1 Sort-based implicit enumeration for OP1

1: Initialize matrix $\boldsymbol{A} = 0$.
2: Step 1: For all beams, find out the maximal K_i elements of all $G_{j,i}$.
3: Step 2: Set $a_{j,i} = 1$ for the selected $G_{j,i}$ in step 1.
4: Step 3: For all users, verify the constraint of C1 and set $a_{j,i} = 0$ except for the maximal $G_{j,i}$.
5: Output optimal matrix $\boldsymbol{A}$.

Algorithm 2 Sort-based implicit enumeration for OP2

1: Initialize matrix $\boldsymbol{B} = 0$.
2: Step 1: For all beams, find out the maximal K_i elements of all $G_{m,i}$.
3: Step 2: Set $b_{m,i} = 1$ for the selected $G_{m,i}$ in step 1.
4: Step 3: For all users, verify the constraint of C1 and set $b_{m,i} = 0$ except for the maximal two $G_{m,i}$.
5: Step 4: update the $\boldsymbol{B}$ according to step 1, 2 and 3 until satisfying all constraints.
6: Output optimal matrix $\boldsymbol{B}$.

To solve OP3, the Dinkelbach algorithm is used. We define $F(L)$ as (51). The designed algorithm is shown in Algorithm 3 within a logarithmic iterative complexity.

$$F(L)_{j,k,i} = B\log_2\left(1 + P_{j,k}G_{j,i} - L\left(\sum_{i' \neq i}^{I}\sum_{j' \neq j}^{J} P_{j',k}G_{j',i} + \sigma^2\right)\right). \tag{51}$$

Algorithm 3 Dinkelbach algorithm for OP3

1: Initialize $L \neq Ans$.
2: **while** $Ans - L \neq 0$ **do**
3: $Ans = L$.
4: Update $F(L)$ for all users and beams.
5: Sort $F(L)$ and get the maximal $\min(K_i, J)$ $F(L)$.
6: Update $p = \sum P_{j,k}G_{j,i}$,
$q = \sum \sum_{i' \neq i}^{I} P_{j',k}G_{j',i} + \sigma^2$ and $L = \frac{p}{q}$.
7: **end while**
8: Calculate and output the optimal results $\boldsymbol{P}$.

The sort-based implicit enumeration algorithm for OP5 is shown in Algorithm 4, whose complexity is $O(M(K_i)^2)$.

Algorithm 4 Sort-based implicit enumeration for OP5

1: Initialize matrix $\boldsymbol{S} = 0$.
2: Step 1: For all associated handover, calculate the their total rate R_m of all sub-channel combination.
3: Step 2: Find out the optimal sub-channel combination $k_{i1} = 1$ and $k_{i2} = 1$ for all associated handover users with the maximal R_m.
4: Step 3: Verify the constraint of C2, keep the maximal one and re-initialize the rest.
5: Step 4: update $\boldsymbol{S}$ according to step 2 and 3 until satisfying all constraints.
6: Output optimal matrix $\boldsymbol{S}$.

To get the results of OP6, we use the gradient descent method [25] according to the solution in Section 4.2. The algorithm we designed is shown in Algorithm 5, and it is run on LEO satellites. The complexity of the designed algorithm is $O(LMNI_nK_n)$, where L is the maximum number of iterations in the proposed algorithm. The algorithm iterates along the gradient and reduces the step length gradually to converge to the optimal result. Once the difference between the latest two iteration results is smaller than the threshold ε_d, the result is close enough to the optimal solution, and the iteration stops.

Algorithm 5 Algorithm for OP6

1: Initialize l_{max}, threshold ε_d and step length $\beta(1)$.
2: Initialize $\lambda_{m,k,i}(1)$, $\mu_{m,k,i}(1)$, $\nu_{m,k,i}(1)$ and $\tau_{m,k,i}(1)$.
3: Initialize $l = 1$, $\xi = 0$, $h(0)$, $P_{k2,m} = P_{\max} - P_{k1,m}$ for all m.
4: **while** $\xi = 0$ **do**
5: **for** $m = 1 : M$ **do**
6: **for** $n = 1 : N$ **do**
7: **for** $i = 1 : I_n$ **do**
8: **for** $i = 1 : K_n$ **do**
9: Update $P^*_{m_{i_n},k_n}(l)$
10: **end for**
11: **end for**
12: **end for**
13: **end for**
14: Calculate $h(l)$.
15: **if** $|h(l) - h(l-1)| \geq \varepsilon_d$ and $l \leq l_{\max}$ **then**
16: **for** $m = 1 : M$ **do**
17: **for** $n = 1 : N$ **do**
18: **for** $i = 1 : I_n$ **do**
19: **for** $i = 1 : K_n$ **do**
20: Update $\beta_\lambda(l+1)$, $\beta_\mu(l+1)$, $\beta_\nu(l+1)$, $\beta_\tau(l+1)$ and $\lambda(1+1)$, $\mu(1+1)$, $\nu(1+1)$, $\tau(1+1)$
21: **end for**
22: **end for**
23: **end for**
24: **end for**
25: $l = l + 1$.
26: **else**
27: $\xi = 1$
28: **end if**
29: **end while**
30: Output optimal power $P^*_{m,k}$.

5. Numerical Results and Discussion

In this section, we carry out simulations to evaluate the improvement of the throughput and fairness brought about by the introduced PD-NOMA-based soft handover scheme in multi-beam LEO-MSS with multiple users and multiple channels. The simulations were implemented using MATLAB R2017a, and the simulation results are presented and analyzed in the following sections.

Table 2. Simulation parameters.

Parameters	Value
Altitude of LEO Satellite	1500 km
V_{LEO}	25,000 km/h
LEO Satellite Antenna η	30
LEO Beam Coverage Radius of 3 dB	100 km
Noise Power Spectral Density	-173 dBm/Hz
Carrier Frequency of Ka Band	30 GHz
B_{total}	240 MHz
Bandwidth of Each sub-channel B	6 MHz
Frequency Reuse Factor N	4
Decode Threshold ε	2 dB
Maximal Transmission Power $P_{\max}$	7 dBW

5.1. System Parameters

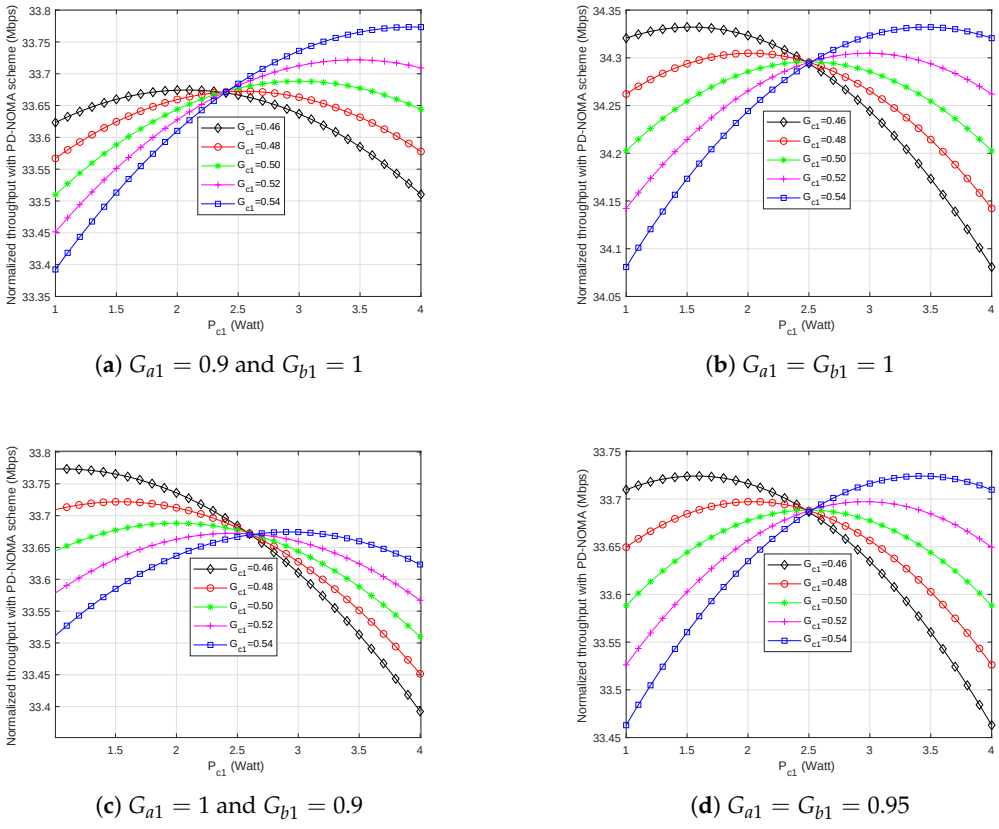
In the simulation, we consider a rectangular region covered by 24 LEO beams, and the users are assumed to follow a uniform distribution (the actual user distribution should be obtained according to the empirical data; the analysis in this paper can be easily extended to arbitrary user distributions.). There are 600 users in total. We focus on the heavy load scenes. The important system parameters are shown in Table 2. The altitude of the LEO satellite with a multi-beam is about 1500 km, and the ground-track speed V_{LEO} is approximately 25,000 km/h. The factor of the LEO satellite antenna η is 30, which means the LEO beam coverage radius of 3 dB is about 100 km. The frequency reuse factor is $N = 4$. The total bandwidth of LEO-ground uplink is 240 MHz. The bandwidth of each sub-channel is $B = 6$ MHz. $P_{\max} = 7$ dBW. The noise power spectral density is -173 dBm/Hz. The carrier frequency of the Ka band is 30 GHz.

5.2. Proposed Uplink PD-NOMA-Based Soft Handover Scheme

To evaluate the proposed uplink PD-NOMA-based soft handover scheme, we carried out a simulation of the scenario in Figure 2. The available bandwidths of MT a and MT b are both 6 MHz, and the handover MT can use the total 12 MHz.

Figure 4 shows the normalized throughput of the PD-NOMA-based soft handover scheme. The normalized throughputs without the PD-NOMA scheme, using the same parameters as in Figure 4a,c, are both 30.27 Mbps. The normalized throughput without the PD-NOMA scheme using the same parameters as in Figure 4b,d are 31.02 Mbps and 30.28 Mbps, respectively. After introducing the PD-NOMA-based soft handover scheme, the throughput can be improved greatly, and one more user can be served. The optimal power allocation results of the handover MT depend on the position of MT a, MT b and the handover MT.

Figure 5 shows the optimal normalized throughput using the PD-NOMA-based soft handover scheme with the optimal power allocation in (17) and the given different channel gains of the MT a, MT b and the handover MT. It gives guidance on the optimal sub-channel allocation and user pairing scheme to achieve larger throughput.



(**a**) $G_{a1} = 0.9$ and $G_{b1} = 1$ (**b**) $G_{a1} = G_{b1} = 1$

(**c**) $G_{a1} = 1$ and $G_{b1} = 0.9$ (**d**) $G_{a1} = G_{b1} = 0.95$

Figure 4. Normalized throughput with PD-NOMA-based soft handover.

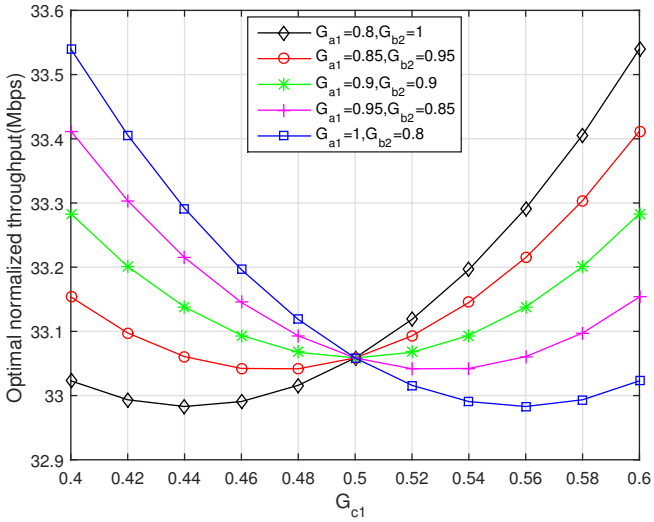


Figure 5. Optimal normalized throughput with PD-NOMA.

5.3. Proposed Handover Optimization

We conducted 100 Monte Carlo simulations, and each instance lasts 1 s and contains 100 transmission time intervals (TTIs). We evaluated the performance of the average number of users being served per beam, the Jain fairness index [28,29] and the average throughput per beam via different strategies and algorithms. We compared the performance of five schemes: the scheme with only OP5, the scheme with both OP5 and OP6, the contrast heuristic method based on the genetic algorithm, the throughput-maximized strategy without PD-NOMA, and the fairness-oriented strategy without PD-NOMA (denoted as "Fairness guarantee" in Figures 6–8). The throughput-maximized strategy prioritizes users

with larger channel gains to maximize system throughput. By contrast, the fairness-oriented strategy assigns higher scheduling priority to users with less cumulative transmitted data, distributing transmission opportunities more evenly across users. This strategy, therefore, prioritizes user fairness over throughput maximization.

Figure 6 shows the average number of users being served per beam under the considered strategies. Without the PD-NOMA scheme, the throughput-maximized strategy serves the fewest users because users with favorable channel conditions are repeatedly prioritized. In contrast, the "Fairness guarantee" strategy assigns higher priority to users with smaller cumulative transmitted data and, therefore, provides transmission opportunities to all users, thereby improving user fairness. After introducing the PD-NOMA scheme, the average number of users being served under the throughput-maximized strategy increases by more than 50%.

Similarly, Figure 7 also shows the 50% increase in user fairness after introducing the PD-NOMA-based soft handover scheme. The fairness performance of the contrast heuristic method based on the genetic algorithm is almost the same as the methods with only OP5 and OP5+OP6, as the allocations before power are the same.

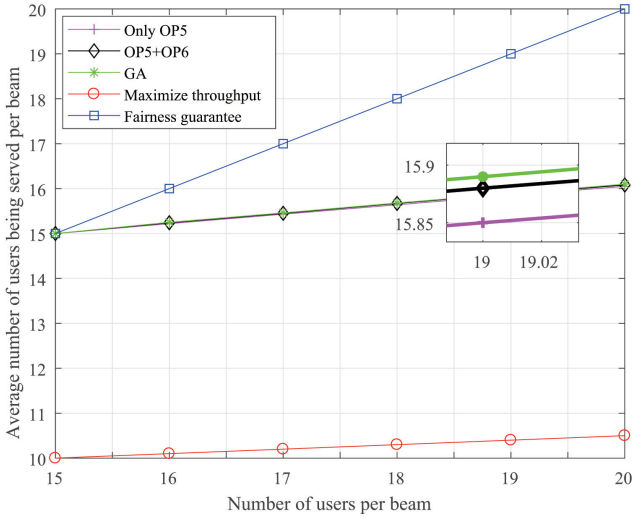


Figure 6. Average number of users being served per beam.

Finally, we evaluated the average throughput of the five strategies and algorithms; the results can be seen in Figure 8. It shows that after introducing the PD-NOMA-based soft handover scheme, the average uplink throughput per beam increases drastically between 11% and 15% with three different algorithms. The contrast heuristic method based on the genetic algorithm provides the best performance in terms of the average uplink throughput. However, its computational complexity and time complexity are too high to be used on the LEO satellites of a practical system. The gradient descent algorithm of OP6 provides about 1.5% less uplink throughput compared with the contrast heuristic method based on the genetic algorithm. However, its complexity is linear, and it can be used on the LEO satellites of a practical system. The power optimization of OP6 provides more than a 2% increase in average uplink throughput.

Generally, the proposed PD-NOMA-based soft handover scheme increases the average uplink throughput to about 15% and increases the average number of users being served to about 50%. The cost is another 50% of the total transmission power at the mobile terminals. In a practical system, the maximal transmission power of the mobile terminals is limited, but the energy of the mobile terminals in this case is not limited and can be supplemented. Therefore, the cost of the proposed PD-NOMA-based soft handover scheme is acceptable. The increases in the number of users being served and the uplink throughput make sense.

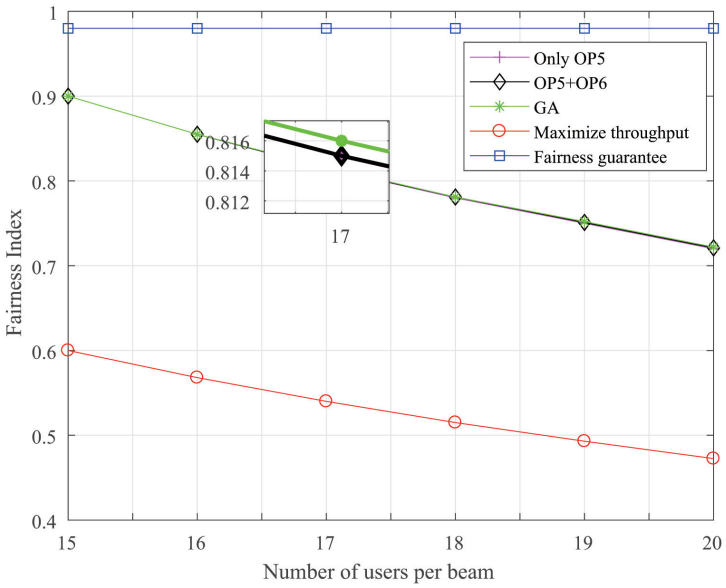


Figure 7. Fairness index.

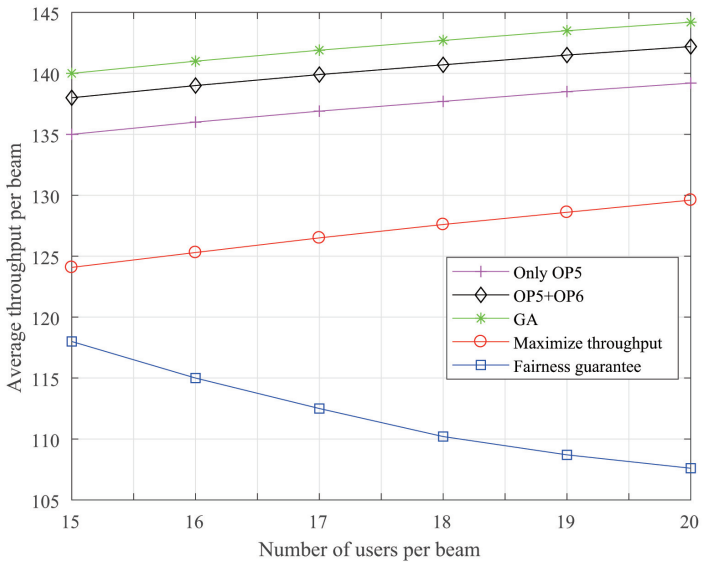


Figure 8. Average throughput per beam.

6. Conclusions and Future Direction

In this paper, we focused on the problem of frequent passive handover in LEO-MSS. We combine a soft handover scheme with uplink PD-NOMA to guarantee QoS for handover users and increase uplink throughput. We analyze the uplink PD-NOMA-based soft handover scheme with three users in two beams and give the closed-form expression of the optimal uplink transmission power allocation. Afterward, we introduce this method into a practical multi-beam LEO-MSS with multiple users and sub-channels, and we formulate the optimization problems to maximize system throughput. Numerical results show that the proposed soft handover scheme based on handover prediction achieves better performance on throughput and fairness with PD-NOMA in heavy loads.

The proposed framework may also be extended to space–air–ground integrated networks to improve uplink throughput and maintain QoS for handover users [30]. Incorporating high-altitude platforms (HAPs) [31] and unmanned aerial vehicles (UAVs) [32] would introduce additional mobility, interference, and resource-coordination challenges, which warrant further investigation. In addition, for terminals without concurrent multi-carrier

uplink capability, the framework can be extended by introducing time-allocation variables and jointly optimizing time- and frequency-domain resources.

Author Contributions: Conceptualization, H.L. and Y.L.; Methodology, H.L. and Y.L.; Validation, C.H. and Y.L.; Investigation, Z.Y. and Y.L.; Writing—original draft, H.L. and Y.L.; Writing—review and editing, H.L. and Y.L.; Visualization, C.H., Z.Y. and Y.L. All authors have read and agreed to the published version of the manuscript.

Funding: This research received no external funding.

Data Availability Statement: The original contributions presented in this study are included in this article. Further inquiries can be directed to the corresponding author.

Conflicts of Interest: Author Hulin Li is the owner of the company Chengdu Heltec Automation Technology Co., Ltd. The remaining authors declare that the research was conducted in the absence of any commercial or financial relationships that could be construed as a potential conflict of interest.

References

1. Azari, M.M.; Solanki, S.; Chatzinotas, S.; Kodheli, O.; Sallouha, H.; Colpaert, A.; Montoya, J.F.M.; Pollin, S.; Haqiqatnejad, A.; Mostaani, A.; et al. Evolution of non-terrestrial networks from 5G to 6G: A survey. *IEEE Commun. Surv. Tutor.* **2022**, *24*, 2633–2672. [CrossRef]
2. Al-Hraishawi, H.; Chougrani, H.; Kisseleff, S.; Lagunas, E.; Chatzinotas, S. A survey on nongeostationary satellite systems: The communication perspective. *IEEE Commun. Surv. Tutor.* **2022**, *25*, 101–132.
3. Pecorella, T.; Ronga, L.S.; Chiti, F.; Jayousi, S.; Franck, L. Emergency satellite communications: Research and standardization activities. *IEEE Commun. Mag.* **2015**, *53*, 170–177. [CrossRef]
4. Li, Y.; Wei, H.; Li, L.; Han, Y.; Zhou, J.; Zhou, W. An extensible multi-Layer architecture model based on LEO-MSS and performance analysis. In Proceedings of the 2019 IEEE 90th Vehicular Technology Conference (VTC2019-Fall), Honolulu, HI, USA, 22–25 September 2019; pp. 1–6.
5. Panigrahy, N.K.; Ghosh, S.C. Analyzing the effect of soft handover on handover performance evaluation metrics under load condition. *IEEE Trans. Veh. Technol.* **2015**, *67*, 3612–3624.
6. Zhao, J.; Liu, Y.; Gong, Y.; Wang, C.; Fan, L. A dual-link soft handover scheme for C/U plane split network in high-speed railway. *IEEE Access* **2018**, *6*, 12473–12482. [CrossRef]
7. Dai, L.; Wang, B.; Ding, Z.; Wang, Z.; Chen, S.; Hanzo, L. A survey of non-orthogonal multiple access for 5G. *IEEE Commun. Surv. Tutor.* **2018**, *20*, 2294–2323. [CrossRef]
8. Islam, S.R.; Avazov, N.; Dobre, O.A.; Kwak, K.-S. Power-domain non-orthogonal multiple access (NOMA) in 5G systems: Potentials and challenges. *IEEE Commun. Surv. Tutor.* **2016**, *19*, 721–742. [CrossRef]
9. Barros, G.; Vieira, J.; Ganhão, F.; Bernardo, L.; Dinis, R.; Carvalho, P.; Oliveira, R.; Pinto, P. A soft-handover scheme for LEO satellite networks. In Proceedings of the 2013 IEEE 78th Vehicular Technology Conference (VTC Fall), Las Vegas, NV, USA, 2–5 September 2013; pp. 1–5.
10. Li, Y.; Zhou, W.; Zhou, S. Forecast based handover in an extensible multi-layer LEO mobile satellite system. *IEEE Access* **2020**, *8*, 42768–42783. [CrossRef]
11. Wang, F.; Jiang, D.; Wang, Z.; Chen, J.; Quek, T.Q.S. Seamless handover in LEO based non-terrestrial networks: Service continuity and optimization. *IEEE Trans. Commun.* **2023**, *71*, 1008–1023. [CrossRef]
12. Han, S.; Li, Z.; Meng, W.; Li, C. Multi-orbit multibeam satellite soft handover strategy based on rate-splitting multiple access. *IEEE Trans. Wirel. Commun.* **2025**, *24*, 6813–6823. [CrossRef]
13. Zhao, M.; Ye, N.; Ouyang, Q.; Jin, Y.; Jin, Y.; Zhao, L. Multi-satellite cooperative communication: Exploiting time asynchrony in non-orthogonal transmissions. *IEEE Trans. Veh. Technol.* **2023**, *72*, 6868–6873. [CrossRef]
14. Zhang, X.; Sun, S.; Tao, M.; Huang, Q.; Tang, X. Multi-satellite cooperative networks: Joint hybrid beamforming and user scheduling design. *IEEE Trans. Wirel. Commun.* **2024**, *23*, 7938–7952. [CrossRef]
15. Yan, X.; An, K.; Liang, T.; Zheng, G.; Ding, Z.; Chatzinotas, S.; Liu, Y. The application of power-domain non-orthogonal multiple access in satellite communication networks. *IEEE Access* **2019**, *7*, 63531–63539. [CrossRef]
16. Yan, X.; Xiao, H.; An, K.; Zheng, G.; Chatzinotas, S. Ergodic capacity of NOMA-based uplink satellite networks with randomly deployed users. *IEEE Syst. J.* **2019**, *14*, 3343–3350.
17. Zhang, X.; Yue, X.; Li, T.; Han, Z.; Wang, Y.; Ding, Y.; Liu, R. A unified NOMA framework in beam-hopping satellite communication systems. *IEEE Trans. Aerosp. Electron. Syst.* **2023**, *59*, 5390–5404. [CrossRef]

18. Ibrahim, A.; Alfa, A.S. Using Lagrangian relaxation for radio resource allocation in high altitude platforms. *IEEE Trans. Wirel. Commun.* **2015**, *14*, 5823–5835. [CrossRef]
19. Balanis, C.A. *Antenna Theory: Analysis and Design*, 2nd ed.; Wiley: New York, NY, USA, 1997.
20. Thornton, J.; Grace, D.; Capstick, M.H.; Tozer, T.C. Optimizing an array of antennas for cellular coverage from a high altitude platform. *IEEE Trans. Wirel. Commun.* **2003**, *2*, 484–492. [CrossRef]
21. Miridakis, N.I.; Vergados, D.D. A survey on the successive interference cancellation performance for single-antenna and multiple-antenna OFDM systems. *IEEE Commun. Surv. Tutor.* **2012**, *15*, 312–335. [CrossRef]
22. Shao, W.; Hu, W.; Huang, X. A new implicit enumeration method for linear 0-1 programming. In Proceedings of the 2008 International Workshop on Modelling, Simulation and Optimization, Hong Kong, China, 27–28 December 2008; pp. 298–301.
23. Yu, Y.; Bu, X.; Yang, K.; Wu, Z.; Han, Z. Green large-scale fog computing resource allocation using joint Benders Decomposition, Dinkelbach Algorithm, ADMM, and Branch-and-bound. *IEEE Internet Things J.* **2018**, *6*, 4106–4117. [CrossRef]
24. Cheung, K.T.K.; Yang, S.; Hanzo, L. Achieving maximum energy-efficiency in multi-relay OFDMA cellular networks: A fractional programming approach. *IEEE Trans. Commun.* **2013**, *61*, 2746–2757. [CrossRef]
25. Tsitsiklis, J.; Bertsekas, D.; Athans, M. Distributed asynchronous deterministic and stochastic gradient optimization algorithms. *IEEE Trans. Autom. Control* **1986**, *31*, 803–812. [CrossRef]
26. Khan, A.A.; Abolhasan, M.; Ni, W.; Lipman, J.; Jamalipour, A. A hybrid-fuzzy logic guided genetic algorithm (H-FLGA) approach for resource optimization in 5G VANETs. *IEEE Trans. Veh. Technol.* **2019**, *68*, 6964–6974. [CrossRef]
27. Souto, V.D.P.; Souza, R.D.; Uchôa-Filho, B.F.; Li, Y. A novel efficient initial access method for 5G millimeter wave communications using genetic algorithm. *IEEE Trans. Veh. Technol.* **2019**, *68*, 9908–9919. [CrossRef]
28. Guo, C.; Sheng, M.; Zhang, Y.; Wang, X. A Jain's index perspective on α-fairness resource allocation over slow fading channels. *IEEE Commun. Lett.* **2013**, *17*, 705–708. [CrossRef]
29. Sediq, A.B.; Gohary, R.H.; Schoenen, R.; Yanikomeroglu, H. Optimal tradeoff between sum-rate efficiency and Jain's fairness index in resource allocation. *IEEE Trans. Wirel. Commun.* **2013**, *12*, 3496–3509. [CrossRef]
30. Chen, Q.; Guo, Z.; Meng, W.; Han, S.; Li, C.; Quek, T.Q.S. A survey on resource management in joint communication and computing-embedded SAGIN. *IEEE Commun. Surv. Tutor.* **2024**, *27*, 1911–1954. [CrossRef]
31. Mohammed, A.; Mehmood, A.; Pavlidou, F.-N.; Mohorcic, M. The role of high-altitude platforms (HAPs) in the global wireless connectivity. *Proc. IEEE* **2011**, *99*, 1939–1953. [CrossRef]
32. Mozaffari, M.; Saad, W.; Bennis, M.; Nam, Y.-H.; Debbah, M. A tutorial on UAVs for wireless networks: Applications, challenges, and open problems. *IEEE Commun. Surv. Tutor.* **2019**, *21*, 2334–2360. [CrossRef]

Disclaimer/Publisher's Note: The statements, opinions and data contained in all publications are solely those of the individual author(s) and contributor(s) and not of MDPI and/or the editor(s). MDPI and/or the editor(s) disclaim responsibility for any injury to people or property resulting from any ideas, methods, instructions or products referred to in the content.